EXPERIMENTAL BALLISTICS AND COMPARATIVE QUANTIFICATION OF NOVEL POLYMER FOAM CORE SANDWICH STRUCTURES

Srikanth Raviprasad[a], Christopher Murzyn[b], Diab Abueidda[b], Jacob Meyer[b], Christopher Kozuch[b], Nick Glumac[b], Iwona Jasiuk[b]*

[a]Department of Aerospace Engineering, University of Illinois at Urbana Champaign, Champaign, IL – 61801
[b]Department of Mechanical Science and Engineering, University of Illinois at Urbana Champaign, Champaign, IL – 61801

*Corresponding author.
Email address: ijasiuk@illinois.edu

Abstract

Regarding protection against ballistic impacts, sandwich structures have shown promising results due to their high rigidity as well as strength to weight ratio. Most popular systems involving low velocity impacts have utilized axially consistent lattice core structures that provided sufficient strength, but proved to be heavier for some applications. Over the years, the focus shifted towards foam core sandwich structures mainly due to their high toughness, high impact strength, and low weight. Although the traditional polyurethane foams and polyvinyl chloride polymers had lower weight compared to stochastic aluminum foams, they had a much lower toughness and could not be used in ballistic applications. As the need for non-conductive and light weight impact resistant structures increased, a significant amount of work was carried out in developing hybrid foam core architectures that aimed to perform better than stochastic closed cell aluminum foams. In this pursuit, this paper evaluates the impact resistance of Aromatic Thermosetting co-Polyester (ATSP) foam core sandwich structures as well as ATSP foam core sandwich structures infused with 3wt% graphene nanoplatelets (GNP), against stochastic closed cell aluminum foam core sandwich structures at velocities ranging from 240m/s to 540m/s. A qualitative as well as the quantitative analysis was performed to compare the materials. The densities of polymer samples were significantly smaller than the aluminum samples. The ATSP as well as ATSP+GNP samples were observed to have much higher adhesion strength than the aluminum samples which exhibited delamination failure. Results of quantitative analysis showed that the ATSP sample also exhibited higher toughness and strength than the aluminum sample at impact velocities ranging between 240-300m/s. This material - being a breakthrough in ballistics

- can be primarily used in applications that require non-conductive materials with extremely high toughness and low density.

Keywords: Ballistic impact; Aromatic Thermosetting co-Polyester (ATSP); Graphene Nanoplatelets (GNP); Foam core sandwich structure

1. Introduction

Impact resistant structures are desired for many applications, and key among these are high speed vehicles, such as aircraft, trains, rockets, and satellites. In 2013, the FAA received 601 reports of wildlife strikes that caused damage, and it is estimated that these strikes cost the aviation industry as much as $937 million [1]. Even hail strikes can cause severe damage to aircraft [2]. Many high-speed trains suffer from similar issues [3]. Rockets and satellites are also vulnerable to impact events. The failure of the Space Shuttle Columbia was due to damage sustained after broken insulating foam impacted the left wing [4]. Non-functioning space debris is putting spacecraft at risk [5,6].

Typically these challenges would be overcome by employing reliable, but heavy materials. However, heavy materials reduce efficiency and increase fuel costs when utilized for vehicles. According to the Bureau of Transportation statistics, the global community burned more than 16 billion gallons of airline fuel at the cost of more than 30 billion dollars in 2015. To put that in perspective, the World Bank estimates that more than half the world's countries have a GDP less than 30 billion dollars.

Clearly, a light-weight structure that provides the same or better impact resistance as heavier alternatives would be highly advantageous. Sandwich structures, where a light-weight core is sandwiched between two high-strength face-sheets, have demonstrated excellent properties in this regard [7]. However, there is still much debate as to the geometric configuration and material constituents used in the construction of these structures.

There are three widely used material systems for the sandwich core. The oldest and most widely used system is that of axially consistent structure, such as a honeycomb or corrugated extrusion. This core type is relatively strong, and its exact geometry can be tightly controlled for optimization, but it is often heavier than other designs [8]–[14]. Recently, cellular and lattice structures enabled by advanced manufacturing techniques have become more common. Lattice cores use significantly less material than honeycombs or corrugation, but they are difficult to manufacture, and they fail abruptly [15]–[17]. This work focuses on the third material system: foams. Foams can be extremely light weight, and many demonstrate excellent energy absorption properties, which makes them a strong candidate for impact resistance [18].

As with the other core systems, most foam cores are composed of aluminum. Aluminum foams are easily manufactured, demonstrate excellent impact resistance, and are relatively light compared to other conventional metals [19]–[24]. However, metals are no longer the only feasible material for impact resistant foams. Polymers have recently become a key interest for impact resistant foam cores, mainly due to their low weight. The two most popular polymers for foam cores are polyurethane and polyvinyl chloride. An advantage of these polymer foams is that they can either be coupled with reinforcement structures, such as rods and lattices, or they can stand alone [25]–[28]. Polymer foams can also be reinforced with additives [29], [30].

Another class of polymers, Aromatic Thermosetting co-Polyester (ATSP) resins, have previously been demonstrated to be thermally stable with high glass transition temperature [31, 32] and ablative character [33]. They also exhibit excellent adhesion to aluminum and titanium with a lap shear strength of up to 15 MPa [34]. Recent work [35, 36] has shown that ATSP may produce hybrid cell (mixed open and closed character) foams with a self-generated blowing agent. The particular chemistry used in this study (CB2AB2) previously demonstrated a compressive strength of 10.52 MPa and Young's modulus of 0.30 GPa, with a density of 0.63 g/cm^3 (relative density of 0.48).

This paper seeks to evaluate the impact resistance of new polymer foam core sandwich structures, one made of Aromatic Thermosetting co-Polyester (ATSP) and another made of ATSP reinforced with graphene nanoplatelets (GNP), and carry out the qualitative and quantitative comparison of its properties against conventional aluminum foam core sandwich structures. Post processing analyses were performed using high speed images at various stages of impact and photographs and radiography images taken after impact, to qualify and quantify the novel sandwich panels.

2. Materials

2.1. Aromatic Thermosetting co-Polyester (ATSP) foam core sandwich

Aromatic copolyester oligomers with carboxylic acid (CB2) and acetoxy functional end groups (AB2) were synthesized via melt oligomerizations at 270°C as in Frich *et al* [31,35,36]. Carboxylic acid-capped CB2 oligomers were produced using an initial monomer feed ratio of 1:3:5:3 trimesic acid : isophthalic acid : 4-acetoxybenzoic acid : biphenol diacetate while acetoxy-capped AB2 oligomers were produced using an initial feed of 1:1:5:4. CB2 and AB2 oligomers have number-average molecular weights of 1760 and 1758 g/mol, respectively.

CB2 and AB2 oligomers were ground such that the powders passed through a 90 μm sieve, weighed, and blended at a weight ratio of 1:1. Blended powders were loaded into a square cavity between two aluminum plates of dimensions 0.12x0.12x0.002m and cured at a temperature of 330°C in a previously described process. For the case of the neat resin foams, 0.058 kg was loaded into the 0.1 m square and 0.0127 m deep cavity. The resulting foam had a density of 4600kg/m^3. Samples reinforced with graphene nanoplatelets (GNPs) were prepared using 25 μm “M-grade” GNP purchased from XG Sciences. These samples were similarly loaded with 0.07 grams of powder with the GNP embodying three weight percent and then cured. The higher loading mass is due to the typically higher density of the GNP-loaded product foam which was found to be 550kg/m^3. Figure 1 illustrates the side view of the ATSP foam core sandwich panel and Figure 2 shows the ATSP foam core sandwich panel infused with GNP.

Figure 1: ATSP foam core sandwich panel.

Figure 2: ATSP foam core sandwich panel infused with 3wt% GNP.

2.2. Aluminum foam core sandwich

Stochastic closed cell aluminum foam core samples of density 600kg/m^3 and 450kg/m^3 were obtained from McMaster Carr and machined to 0.1x0.1x0.0127m and 0.0254m to prepare 0.0127m and 0.0254m thick foam cores, respectively. These samples were used as the core material between two aluminum 6061 plates, each with dimensions of 0.12x0.12x0.002m. The resulting panel was bonded together using Loctite® Epoxy Heavy Duty two-part adhesive, which consists of an epoxy resin and a hardener due to its high tensile and compressive shear strengths. The sample was then cured at room temperature for 24 hours so as to be fully operational. Figure 3 shows the 0.0127m thick aluminum foam core sandwich panel.

Figure 3: Half-inch thick aluminum foam core sandwich panel.

3. Experiments

The samples were tested at the University of Illinois at Urbana-Champaign research laboratories using a powder gun setup confined within a sound proof chamber. The experimental arrangement and boundary conditions are explained in the following sections.

3.1. Experimental setup

The ballistic testing for this study was conducted using a modified 0.308 rifle barrel. The barrel was retrofit with a custom breech loading apparatus to accommodate a broad range of gunpowder charge. Commercial rifle and pistol powder were ignited by mechanically switching a 50V source across a 0.00025m nickel-chromium (nichrome) wire. The hemispherical nose shaped projectile was made of an aluminum 6061 alloy. It was machined to a length of 0.0254m and a diameter of 0.00763m.

Bullet velocity was measured using two electrical trip wires separated by a fixed distance. When the bullet broke the trip wires, the voltage change was recorded on a PicoScope 3424 digital oscilloscope. A Berkeley Nucleonics Corporation, model 565 delay generator was externally triggered from the voltage rise of the leading trip wire. The delay generator was used to initiate the flash and the high-speed camera. Impacts were imaged using a Vision Research, Phantom v5.2 CMOS camera coupled with a 0.05m, f/1.2 Nikkor lens. They were illuminated with a PowerLight 2500 DR flash lamp. The Phantom camera was running at 16,806 frames per second (59.50 μs period) with a 2 μs exposure time. This speed was achieved by setting a resolution to 400 x 104 pixels. Figure 4 shows the schematic of the experimental setup.

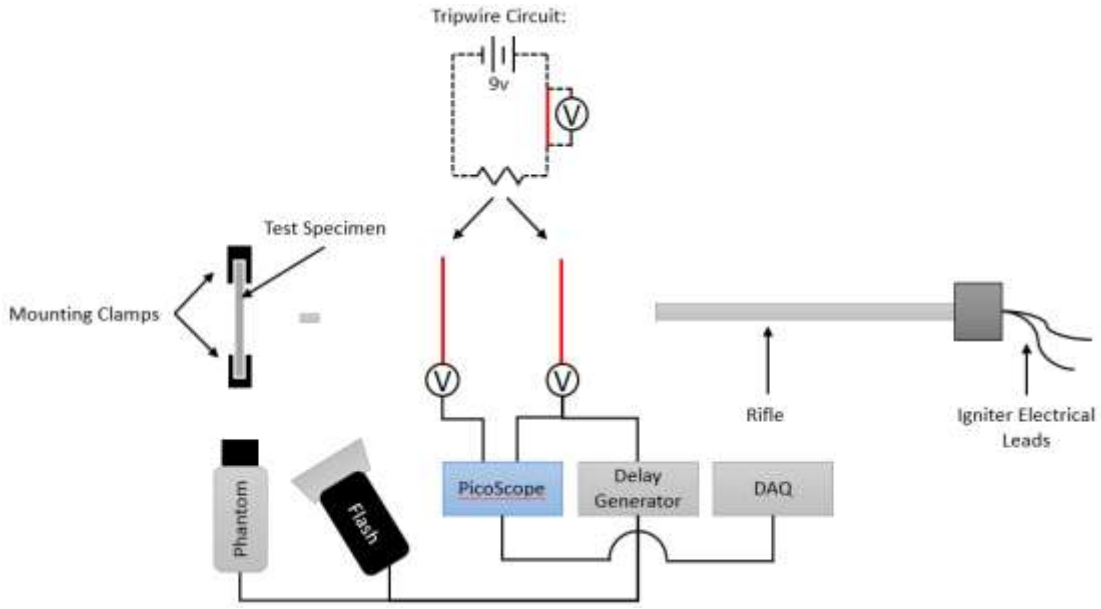

Figure 4: Schematic of the experimental setup.

The foam core sandwich panels were positioned between two custom designed L-clamps which were bolted onto an optical table as shown in Figure 5. Figure 5 also shows an image captured by the high speed video, with a 0.00482m thick aluminum plate and a fiducial marker so as to give a better idea about the resolution and the field of view. This setup was designed such that it could accommodate samples of any thickness ranging from 0.002m to 0.028m. This assembly formed the boundary conditions with zero displacements in all three directions for the problem. As the samples were sandwiched between 2 L-clamps bolted to each other, they were held tight and constrained in all three degrees of translation freedom and all three rotational degrees of freedom.

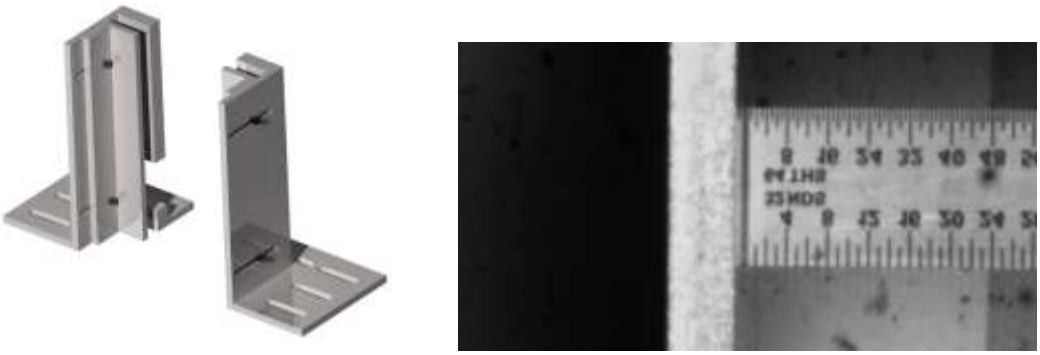

Figure 5: L-clamps used to hold the sample and a high speed image with a fiducial marker.

3.2. Test cases

As explained in the previous sections, three types of foam core sandwich samples were prepared to compare and quantify their impact resistance behavior. High-speed images were captured at 13,071 frames per second to get a better understanding of the projectile and target interaction during impact as well as any delamination behavior that would follow. Table 1 enumerates the test cases, sample types, and bullet velocities at impact.

Table 1: Test cases of different materials corresponding to respective velocities

Sample ID	Sample Type	Foam core thickness (m)	Velocity (m/s)
S-1	Aluminum foam core sandwich	0.0254	292.9
S-2	Aluminum foam core sandwich	0.0254	403.3
S-3	Aluminum foam core sandwich	0.0127	554.2
S-4	ATSP foam core sandwich	0.0127	240.0
S-5	ATSP + GNP foam core sandwich	0.0127	271.0
S-6	ATSP + GNP foam core sandwich	0.0127	344.7

3.2.1. Aluminum foam core sandwich

Aluminum foam core sandwich panels with foam core thicknesses 0.0127m and 0.0254m were impacted at different velocities as mentioned in Table 1. There was no predefined relation between the amount of gunpowder used and the velocity imparted to the projectile because the amount of gunpowder that undergoes combustion in a particular shot is unpredictable. Efforts were made to maintain the same test conditions throughout the experimental domain so as to get a better hold on the precision of the analysis.

Figures 6 through 8 show the high-speed images of the three above mentioned samples before, during and after impact. These photographs also depict the damage response of panels, including the aspects of possible penetration or perforation and delamination.

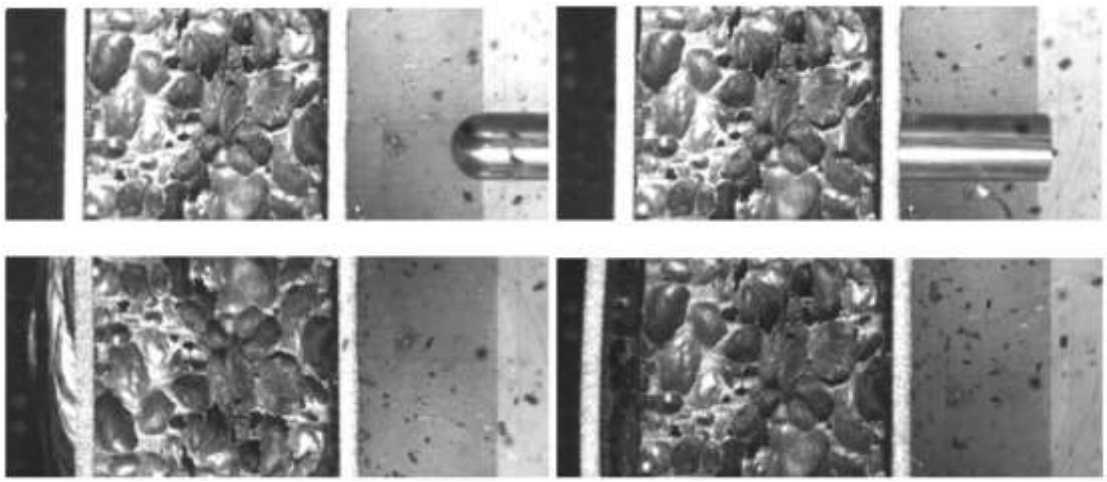

Figure 6: High-speed time lapse image of test case corresponding to sample S-1, ordered from top left to bottom right - 292.9m/s.

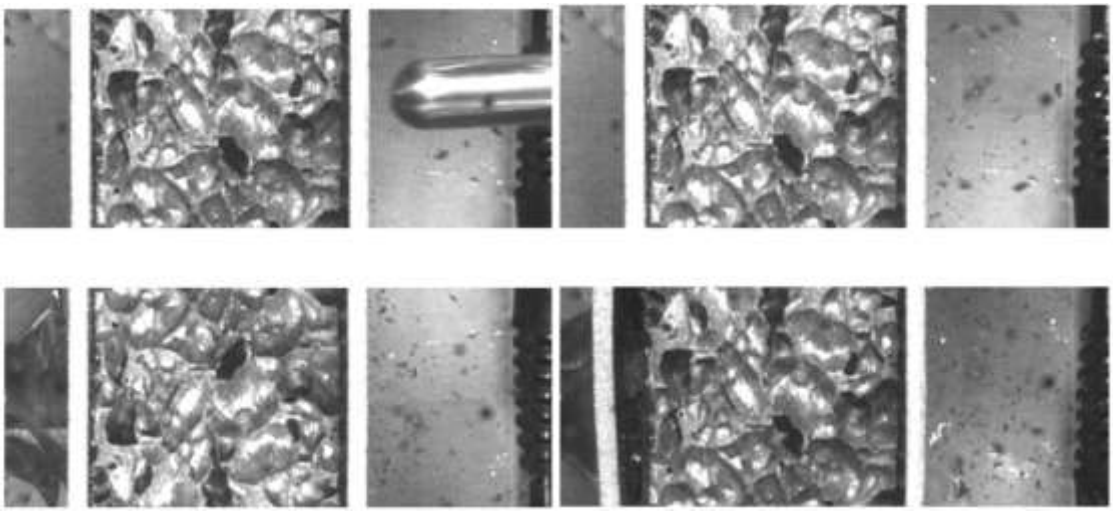

Figure 7: High-speed time lapse image of test case corresponding to sample S-2, ordered from top left to bottom right – 403.3m/s.

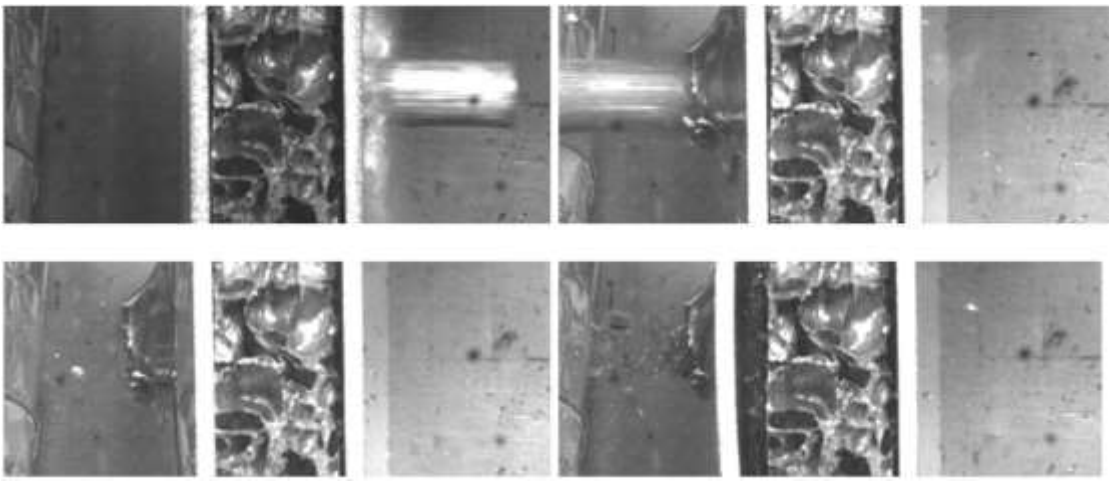

Figure 8: High-speed time lapse image of test case corresponding to sample S-3, ordered from top left to bottom right – 554.2m/s.

3.2.2. ATSP foam core sandwich

ATSP Foam core sample of 0.0127m thickness was impacted against an aluminum projectile at a velocity of 240.0m/s. Figure 9 shows the time lapse images of the impact phenomenon, covering the pre-contact, impact and post-impact stages for this case.

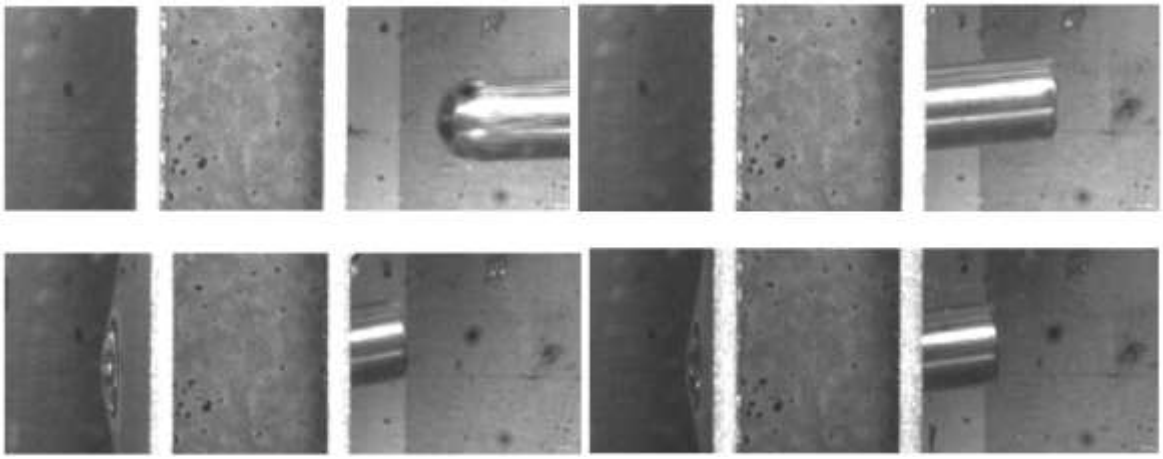

Figure 9: High-speed time lapse image of test case corresponding to sample S-4, ordered from top left to bottom right – 240.0m/s.

3.2.3. ATSP with GNP

Two ATSP Foam core samples of 0.0127m thickness infiltrated with GNP were impacted against aluminum projectiles at velocities mentioned in Table 1. Figures 10 and 11 show the time lapse images of the impact phenomenon, covering impact and post-impact stages.

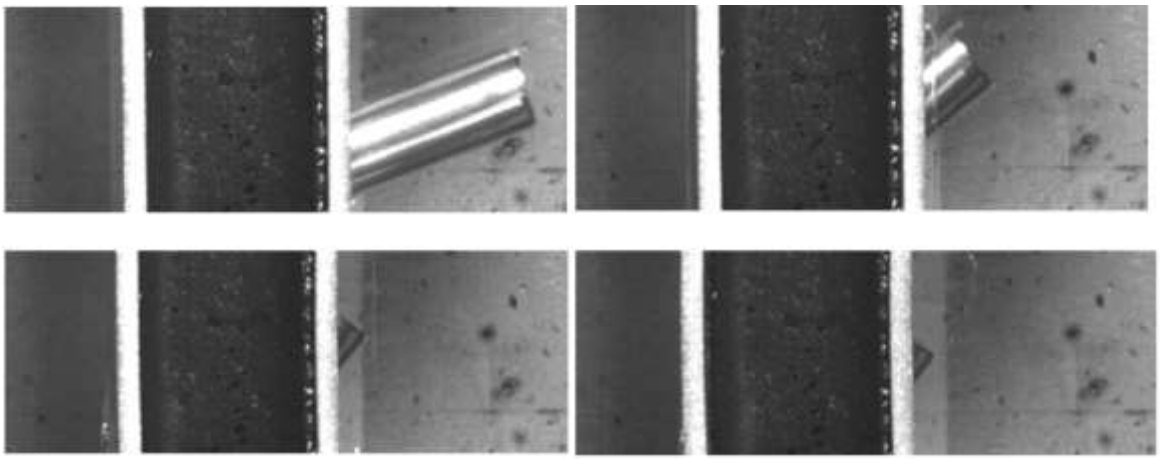

Figure 10: Highspeed time lapse image of test case corresponding to sample S-5 ordered from top left to bottom right – 271.0m/s.

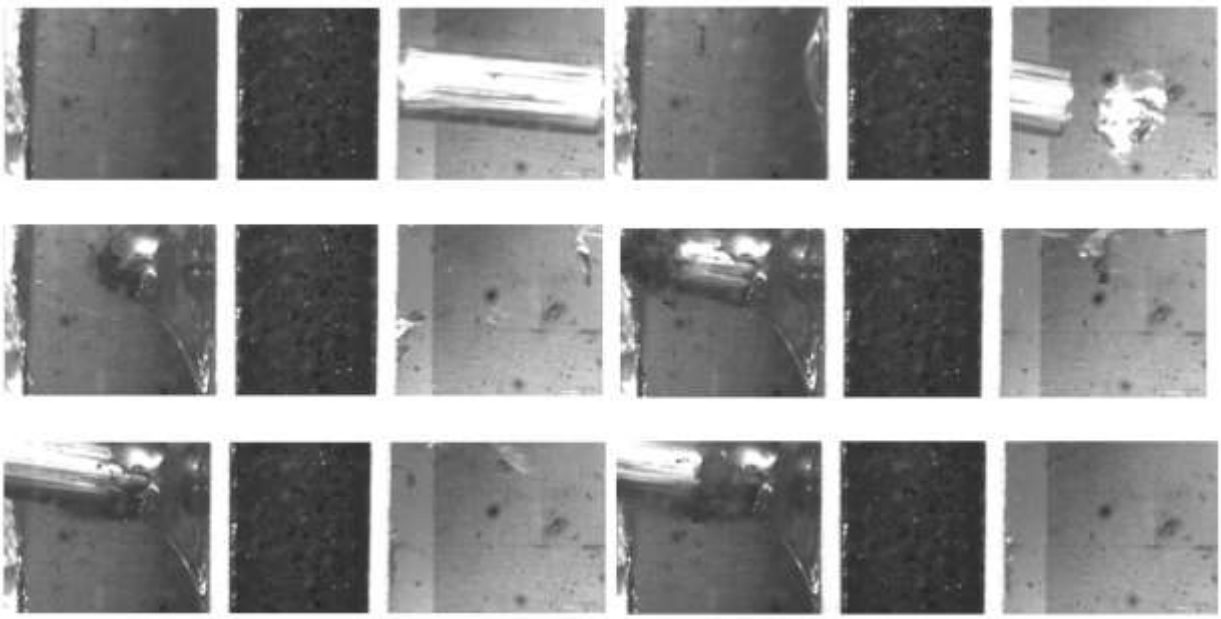

Figure 11: High-speed time lapse image of test case corresponding to sample S-6, ordered from top left to bottom right – 344.7 m/s.

4. Results and discussion

Radiographic imaging of the six samples was carried out after impact testing. It was observed from experiments that samples S-1, S-4, and S-5 were subjected to just penetration and not perforation type of damage. However, samples S-2, S-3, and S-6 experienced perforated failure. The penetrating and perforating cases are separately analyzed in section 5. This section discusses the qualitative analysis and damage characterization of the six samples based on visual inspection of the x-ray images as well as the high-speed images shown earlier.

4.1. Aluminum foam core sandwich

After impact high definition images and radiography images of samples S-1, S-2, and S-3 are shown below. Samples S-1 through S-3 are separately analyzed to qualify their post-impact behavior.

4.1.1. Post-impact qualitative analysis of Sample S-1

The projectile pierced through the front face of the panel and its kinetic energy was completely dissipated into strain and damage to the aluminum foam core, as seen in Figure 12. The bullet carries very low velocity as it impacts the back face of the sample, causing a bulging effect and hence not perforating it. Figure 13 shows the x-ray image of the sample after impact. One can see the bullet being stuck in the sample and causing an apparent bulge in the back plate of the panel. The damage also included the delamination of the panel on its back face due to the fact that the toughness of the epoxy used between the panels was significantly lower than the energy dissipated in the form of damage. Delamination, being a critical failure phenomenon in sandwich structures and composite laminates, proves to be a major factor that could question the impact-worthiness of a target designed for impact resistance.

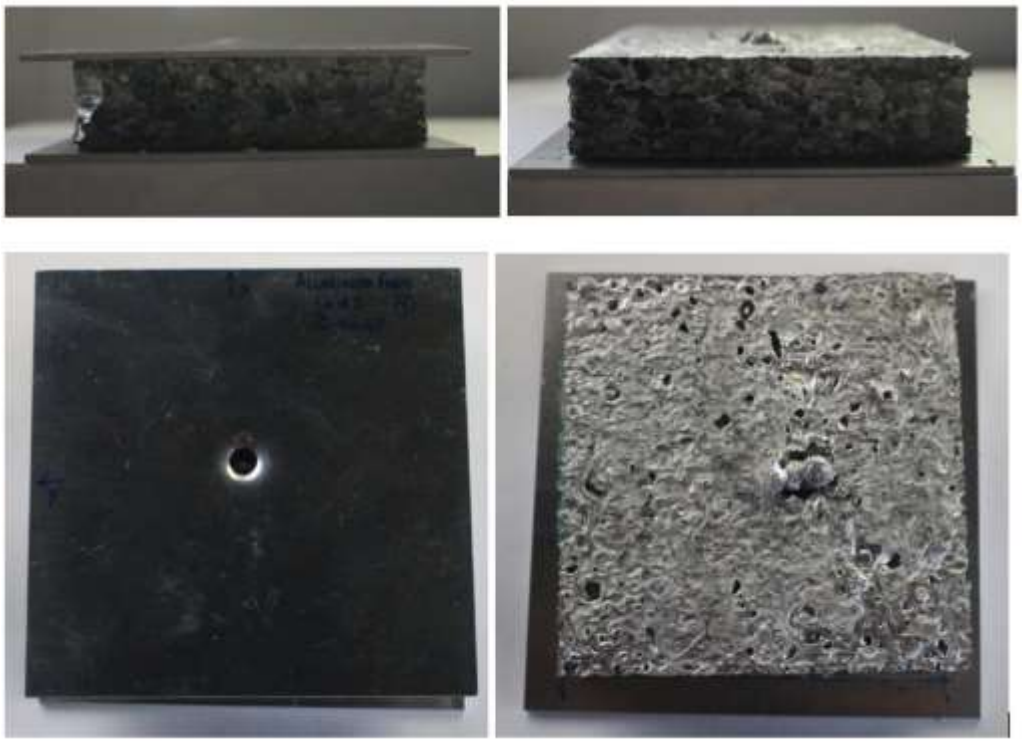

Figure 12: Post-impact images of sample S-1.

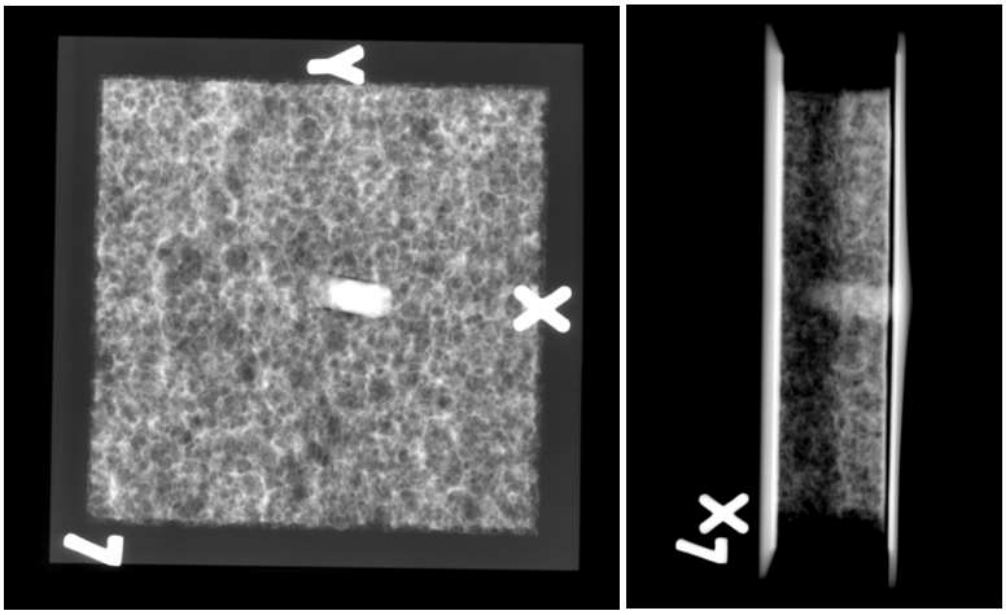

Figure 13: Post-impact radiography images of sample S-1.

4.1.2. Post-impact qualitative analysis of Sample S-2

Figures 14 and 15, show the damage characteristics of sample S-2 when impacted by a projectile at 403.3m/s. The projectile had a finite residual velocity and perforated the sample leading to a pure petaling type of damage. Partial delamination was observed and the adhesive nature of the rear aluminum plate with the foam was compromised. Furthermore, the figures also depict the top view of the sample that experienced petaling failure and the shape of the projectile after impact. One can also ascertain from the x-ray images in Figure 16 that the foam core experienced localized damage even at such high velocities and most energy was dissipated in deforming the rear plate.

Figure 14: Post-impact side view image of sample S-2.

Figure 15: Post-impact top and bottom views of sample S-2.

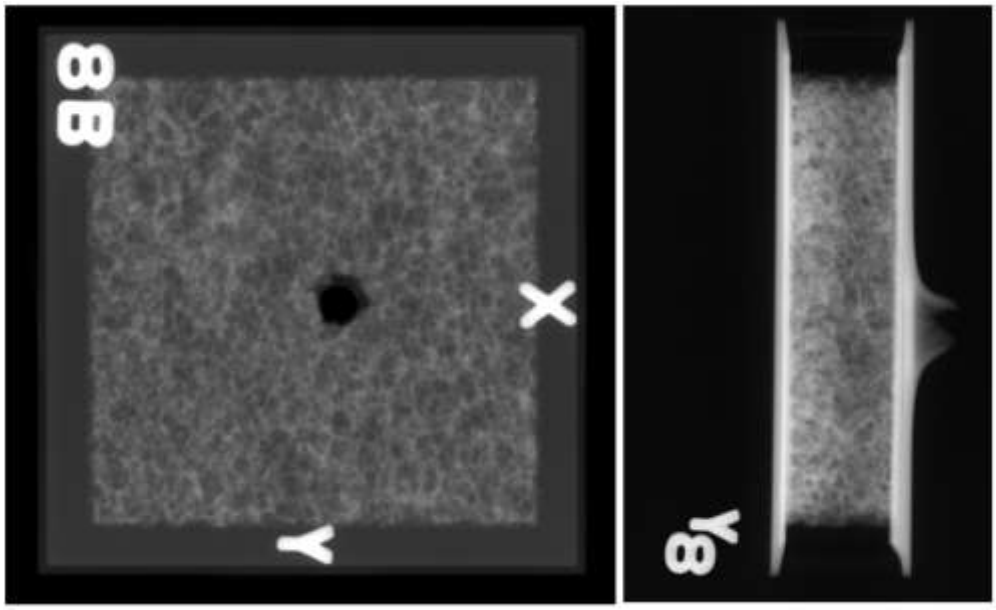

Figure 16: Post-impact radiography images of sample S-2.

4.1.3. Post-impact qualitative analysis of Sample S-3

Sample S-3 experienced a semi petaling-plugging nature of damage when impacted by a projectile moving at a velocity of 554.2m/s. While the projectile could not be recovered after impact, one could observe the partial fragmentation of the projectile and target from the high-speed images shown earlier in Figure 8. This sample also experienced partial delamination and the adhesive strength was faintly compromised because the partial loss in kinetic energy of the projectile was completely dissipated into strain and damage to the aluminum foam and plates. The epoxy holding the panels together absorbed a finite amount of energy that only caused a partial delamination. Figures 17 and 20 depict the post-impact images of sample S-3 and Figure 19 represents the post-impact radiography images of sample S-3.

Figure 17: Post-impact side view image of sample S-3.

Figure 18: Post-impact top and bottom views of sample S-3.

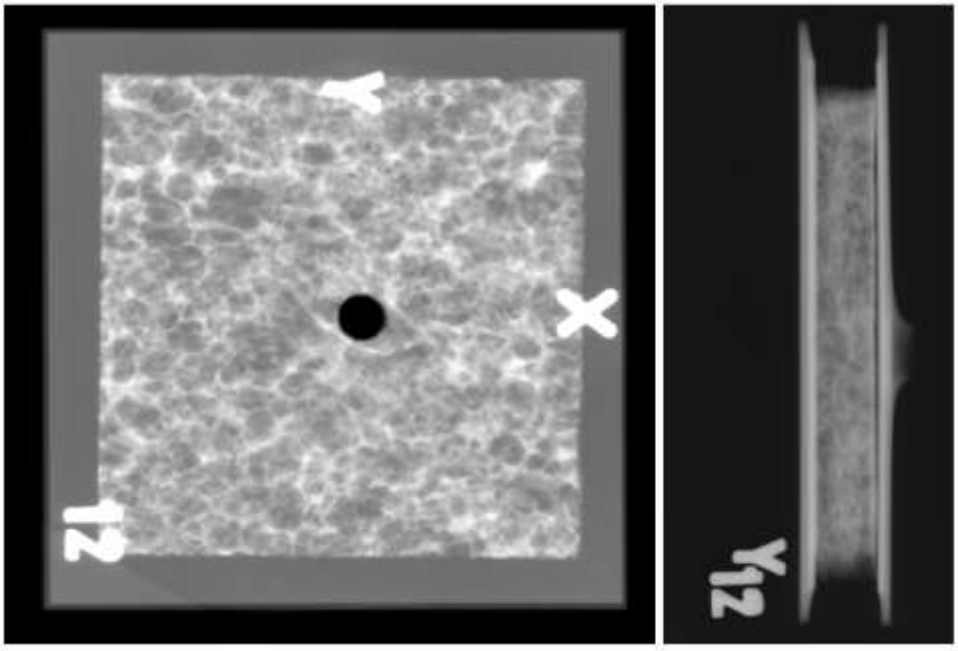

Figure 19: Post-impact radiography images of sample S-3.

4.2. ATSP foam core sandwich

4.2.1. Post-impact qualitative analysis of Sample S-4

The pure ATSP foam core sample was impacted by a projectile moving at 240.0m/s. This sample had superior performance to the aluminum foam core samples when compared over several parameters. The first and foremost criterion where the ATSP foam core performed better than aluminum was in adhesion strength. As seen from high-speed images in Figure 9, the sample did not experience any delamination failure. Post-impact qualitative analysis of the foam also revealed that the panels were intact and adhesion strength was not affected. Furthermore, the sample exhibited high rigidity, stiffness, as well as toughness, which aided in containing the projectile, causing only penetration and not perforation. The projectile got embedded in the sample and caused an insignificant dent on the rear aluminum plate, representing a bulging characteristic. One can also observe the extent of penetration of the projectile from the x-ray images in Figure 22. This behavior of ATSP foam core sandwich did not only prove to be superior to aluminum foam core sandwich in energy absorption, but also redefined the metrics in which post-impact quantitative analysis between these variants had to be performed. This is explained in the next section. Figures 20 and 21 depict the post-impact images of sample S-4.

Figure 20: Post-impact side view image of sample S-4.

Figure 21: Post-impact top and bottom views of sample S-4.

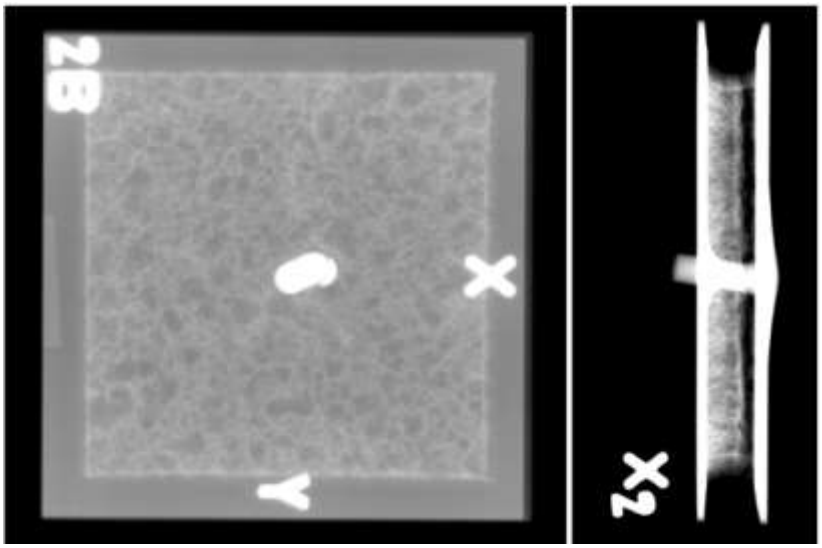

Figure 22: Post-impact radiography images of sample S-4.

4.3. ATSP foam core sandwich with 3wt% GNP

4.3.1. Post-impact qualitative analysis of Sample S-5

The projectile approached the target at a velocity of 271.06m/s, being inclined at an angle of 16.5 degrees, as seen in Figure 10. However, it should be noted that the centroid of the bullet traveled horizontally, hence ruling out any possible inferences that the impact was oblique. It was concluded that the projectile did not establish a roll stability after it exited the barrel, which caused it to wobble as it

approached the target at such a high velocity. Being a derivative of the ATSP foam core sample, sample S-5 did prove to have a high adhesion strength that prevented any delamination from occurring. The sample also successfully contained the projectile within the foam, hence causing only penetration and not perforation. Hence, it was inferred that the kinetic energy of the projectile traveling at a velocity of 271.0m/s was absorbed by the sandwich panel, leaving behind a bulge on the rear plate. Figures 23 and 24 depict the post-impact images of sample S-5 and Figure 25 represents the post-impact radiography images of sample S-5.

Figure 23: Post-impact side view of sample S-5.

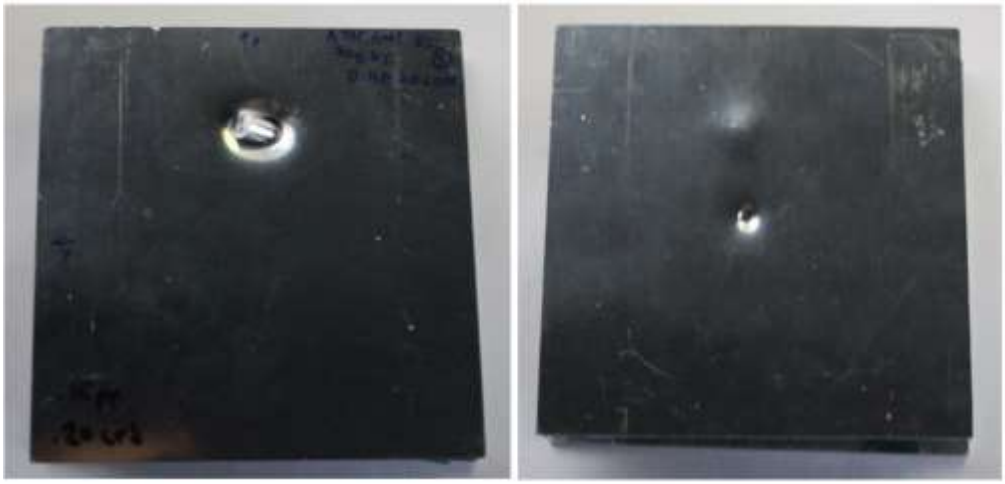

Figure 24: Post-impact top and bottom views of sample S-5.

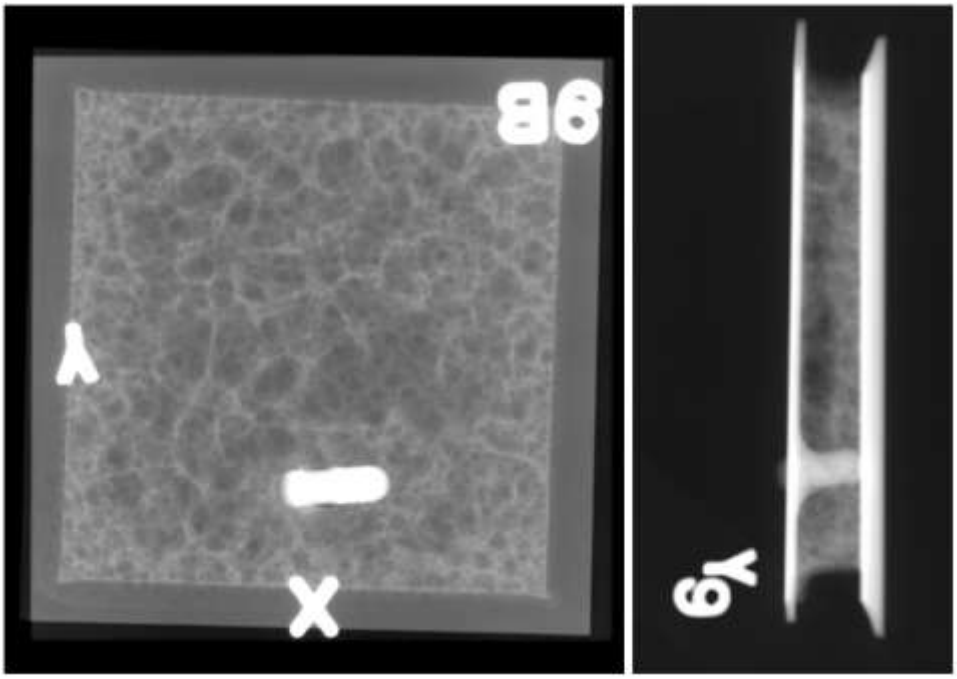

Figure 25: Post-impact radiography images of sample S-5.

4.3.2. Post-impact qualitative analysis of Sample S-6

Sample S-6 is a perfect example of the damage being characterized as a combined plugging and petaling behavior, as seen in Figure 26. The ATSP sample infiltrated with 3wt% GNP performed fairly well when it came to absorbing the kinetic energy of the projectile. A more detailed analysis of the quantification is presented in the next section. Here, a complete perforation of the sample was observed. The projectile first punched through the front face of the panel, displacing a hemispherical slug due to the adiabatic shearing effects along the periphery of the damage region. Furthermore, it pierced through the rear plate, causing high tensile deformation resulting in petaling of the sample. Also, the panel remained intact after impact, which led to an inference that there was no delamination due to the high adhesion strength of ATSP. Figures 26 and 27 depict the post-impact images of sample S-6 and Figure 28 represents the post-impact radiography images of sample S-6.

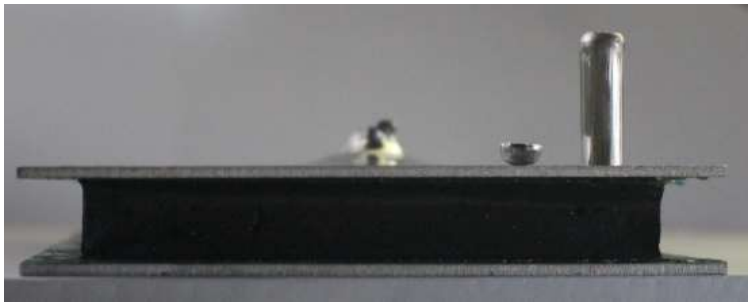

Figure 26: Post-impact side view of sample S-6.

Figure 27: Post-impact top and bottom views of sample S-6.

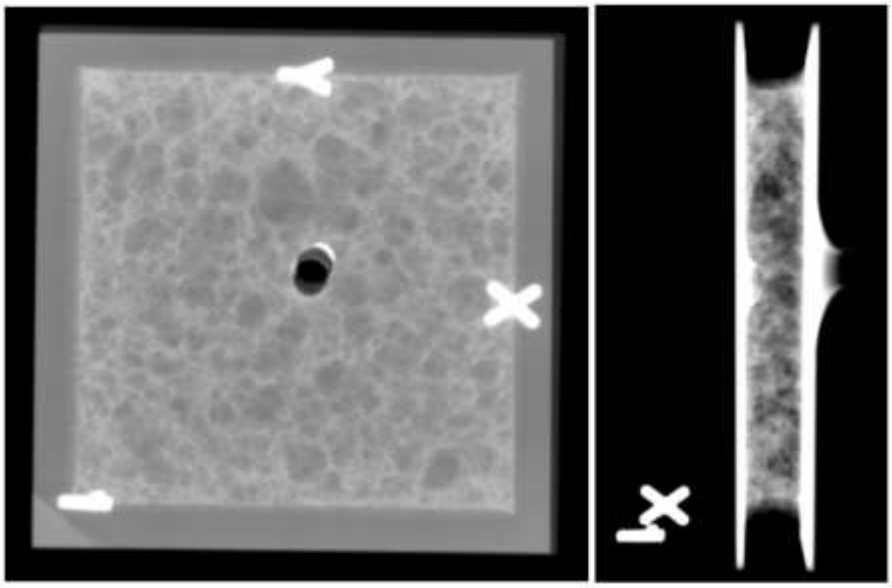

Figure 28: Post-impact radiography images of sample S-6.

4.4. Comparative quantification

Six samples were analyzed for post-impact behavior in qualitative as well as quantitative approaches. The previous section involved qualitative analysis based on damage characterization from after impact images as well as x-ray data. This section contains quantitative analysis of the six samples to compare their performance against ballistic impacts. As mentioned in the previous section, three samples experienced penetration only damage, and three samples experienced perforation damage.

The comparative quantification of the penetrated and perforated samples was done separately due to the unavailability of a common platform for their comparison. The main variables in this impact experiments were: density of foam (ρ), Mach number of projectile (M), extent of deformation in the panel due to penetration (δ), characteristic thickness of the foam core (t = 0.5 and 1 for 0.0127m and 0.0254m samples, respectively), and the inner diameter of the petaling damage caused on the rear plate of the samples (φ). Figures 29 and 30 represent plots that depict the quantitative comparison of samples of various densities plotted against a deformation parameter that has the units of length. The ideal behavior would correspond to a material that relatively has a lower density and yet has a low strain or deformation from damage.

4.4.1. Penetration

The deformation parameter mentioned earlier has the units of length. This parameter has the deformation and characteristic thickness being normalized by the Mach number so that these samples can be compared to one graph in spite of being subjected to impact at different velocities. Samples S-1, S-4 and S-5 underwent penetration type of damage. In this case, the deformation value (δ) was considered as the total extent deformation of the sample due to penetration, measured from the front face of the sample. Measurements were made on the x-ray images obtained after impact. Figure 29 represents the quantification plot for samples S-1, S-4, and S-5 that exhibited penetration damage.

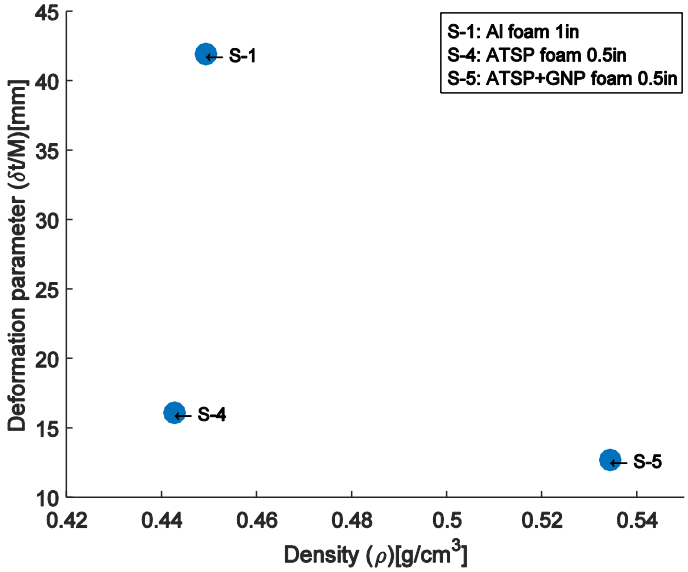

Figure 1: Quantification plot for samples S-1, S-4, and S-5 that exhibited penetration damage.

Sample S-4 had the lowest density of the three samples shown with a value of 442.7kg/m^3, followed by sample S-1 of density 449.1kg/m^3 and S-5 with the highest density of 534.3kg/m^3, as seen in Figure 29. The general notion in mechanics of materials would follow the fact that the total deformation along the normal direction due to impact is inversely proportional to the density of the material. The higher the material density, the lesser the deformation along the normal direction and vice versa. Hence, any material that has lowest density and experiences least damage would be plotted closest to the origin and would appear to be the ideal material to resist ballistic impacts. This idea is well established by the behavior of samples S-1 and S-5 in the above plot. Sample S-5 with the 0.0127m thick ATSP+GNP foam core has 19% more density compared to sample S-1 with 0.0254m thick aluminum foam core but experiences 69.6% less deformation than sample S-1. However, the sample S-4 with 0.0127m thick ATSP foam core has only 1.4% lower density than the sample S-1 but experiences 61.5% less deformation than sample S-1. This behavior implies that the densification region from plastic deformation, and hence the toughness of ATSP foam, is higher than of an aluminum foam core of equivalent geometric parameters. Moreover, sample S-4 has density and deformation characteristics that put it closest to the origin in Figure 29. Hence, it can be concluded that ATSP foam core sandwich is much more effective in ballistic protection than aluminum as

well as ATSP + GNP foam core sandwich under penetrating ballistic impact conditions for applications where minimizing density is the number one priority. Hence the ATSP foam core sandwich is more efficient in energy absorption for ballistic phenomena. Such an observation was also reported by Hassan *et al* [37] and Nasirzadeh *et al* [38] where the authors concluded that foam cores with lesser density absorb more energy and minimize damage in high energy impact and blast impact applications. However, if applications minimizing deformation are the number one priority, one can conclude that ATSP foam core sandwich infused with 3wt% GNP performs few orders of a magnitude better than conventional aluminum foam core sandwich and also faintly better than ATSP foam core sandwich.

4.4.2. Perforation

The deformation value (φ) in the deformation parameter for the perforation type of damage was considered to be the inner diameter of the petaling damage caused on the rear aluminum plate of the sample. This deformation value and characteristic thickness were normalized by the Mach number so that these samples can be compared under one graph in spite of being subjected to impact at different velocities. Samples S-2, S-3 and S-6 underwent perforation type of damage. Measurements were made on the x-ray images obtained after impact. Figure 30 represents the quantification plot for samples S-2, S-3 and S-6 that exhibited perforation damage.

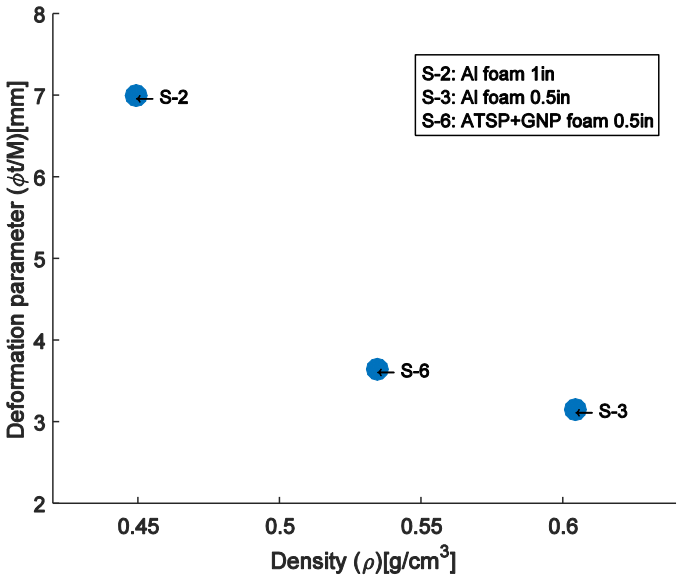

Figure 30: Quantification plot for samples S-2, S-3, and S-6 that exhibited perforation damage.

Sample S-2 had the lowest density of the three samples shown with a value of 44k9.1g/m^3, followed by sample S-6 of density 534.4kg/m^3 and S-3 with the highest density of 604.3kg/m^3, as seen in Figure 30. As mentioned in the previous section, the general notion follows the fact that higher the density of the material, lower is the deformation and vice versa.

The sample S-3 is 34.5% denser than sample S-2, but it experienced 54.8% less deformation than sample S-2, as seen in Figure 30. Similarly, sample S-6 is 19.0% denser than sample S-2, but it experienced 47.8% less deformation when compared to sample S-2. The real argument arises when sample S-6 is compared against sample S-3. The 0.0127m thick ATSP+GNP foam core sandwich is 11.6% less dense than the 0.0127m thick aluminum foam core sandwich but experienced 15.5% more deformation than the latter. From observing a decrease in deformation from an almost equivalent increase in density, one can infer that the aluminum foam core sandwich was more effective than an ATSP+GNP foam core sandwich in high-velocity impact cases. Table 2 summarizes all the 6 test cases as well as quantifies the damage in terms of the ratio of deformation parameter to density.

Table 2: Summary of test results for the 6 samples

Sample ID	Sample Type	Foam core thickness (m)	Velocity (m/s)	Damage Characteristics	Deformation Parameter/Density (Relative values without dimensions)
S-1	Aluminum foam core sandwich	0.0254	292.9	Penetration	8.030
S-2	Aluminum foam core sandwich	0.0254	403.3	Perforation	18.48
S-3	Aluminum foam core sandwich	0.0127	554.2	Perforation	17.04
S-4	ATSP foam core sandwich	0.0127	240.0	Penetration	5.150
S-5	ATSP + GNP foam core sandwich	0.0127	271.0	Penetration	3.800
S-6	ATSP + GNP foam core sandwich	0.0127	344.7	Perforation	13.84

5. Conclusions

In this work, the authors evaluated the impact resistance of new polymer foam core sandwich structures, one made of Aromatic Thermosetting co-Polyester (ATSP) and another made of ATSP reinforced with graphene nanoplatelets (GNP), and carried out a quantitative comparison of its properties against conventional aluminum foam core sandwich structures. Qualitative and quantitative aspects of post processing analysis were performed using high-speed images at various stages of impact, radiography images after impact, and photographs of samples taken after impact. A few conclusions were derived from this work:

a) The ATSP samples, as well as ATSP infused with GNP, exhibited much superior adhesion properties when compared to aluminum foam core sandwich, when subjected to both, low (<300m/s) and high velocity

(>300m/s) ballistic impacts. The aluminum foam samples experienced delamination while the polymer samples were intact.

b) ATSP foam core sandwich panel had the lowest density and yet experienced very less deformation when subjected to low velocity ballistics (<300m/s). ATSP+GNP performed marginally better than ATSP samples, but they had much higher density.

c) For low velocity ballistics involving penetration (<300m/s), polymer foams exhibited much better performance compared to aluminum foams due to their high adhesive strength and toughness. For higher velocities involving perforation (>300m/s), 0.0127m thick aluminum foam core sandwich panels performed marginally better than polymer foam core panels.

d) There was always a dearth of impact resistant materials in non-conductive ballistic applications where minimizing density was a priority. This work introduces a novel polymer sandwich structure (non-conductive) that has much lower density when compared to equivalent aluminum foam and yet has very high toughness and impact strength.

6. Future scope of work

As ATSP is quite new to the field of ballistics, this polymer foam core sandwich could be fabricated with several different configurations. For example, one could vary the amount of GNP infused in ATSP polymer foam so as to analyze its behavior and possibly determine an optimum amount of GNP that could maximize the impact strength of the foam. This could possibly be used in applications involving high velocity ballistics. Moreover, due to its superior adhesion properties, ATSP could also be used as an adhesive between the components of an aluminum foam core sandwich structure. The resulting sample could then be analyzed and compared with pure ATSP foam core sandwich structures for ballistic response.

7. Acknowledgements

The authors are grateful to Dr. John Popovics and his group at the University of Illinois, for their assistance in obtaining x-ray images of samples after impact. The authors are also thankful to Mete Bakir, graduate student at the University of Illinois, for his valuable suggestions. Efforts of Cliff Gulyash and his group at the machine shop of Mechanical Science and Engineering are also acknowledged. Finally,the authors gratefully acknowledge funding from the National Science Foundation (NSF) I/UCRC grant (IIP-1362146). The findings, conclusions and recommendations expressed in this manuscript are those of the authors and do not necessarily reflect the views of the NSF.

8. References

[1] R. A. Dolbeer, S. E. Wright, J. R. Weller, A. L. Anderson, and M. J. Begier, "Wildlife strikes to civil aircraft in the United States 1990–2013," Washington, D.C., 2014.

[2] T. F. Schoenherr, "Calculating the Impact Force of Supersonic Hail Stones Using SWAT-TEEM," in 33rd IMAC, A Conference and Exposition on Structural Dynamics, 2015, vol. 9, pp. 67–79.

[3] G. Belingardi, M. P. Cavatorta, and R. Duella, "Material characterization of a composite-foam sandwich for the front structure of a high speed train," Compos. Struct., vol. 61, no. 1–2, pp. 13–25, 2003.

[4] NASA, "Columbia Crew Survival Investigation Report," 2008.

[5] T. Ebisuzaki *et al*., "Demonstration designs for the remediation of space debris from the International Space Station," Acta Astronaut., vol. 112, pp. 102–113, 2015.

[6] M. Nayyar, S. Raviprasad, V. Chandrasekaran, and Y. V. Gupta, "Protection of Spacecraft from Space Environmental Effects," in 64th International Astronautical Congress, 2013.

[7] H. G. Allen, Analysis and Design of Structural Sandwich Panels: The Commonwealth and International Library: Structures and Solid Body Mechanics Division. Elsevier, 2013.

[8] A. Akatay, M. Ö. Bora, O. Çoban, S. Fidan, and V. Tuna, “The influence of low velocity repeated impacts on residual compressive properties of honeycomb sandwich structures,” Compos. Struct., vol. 125, pp. 425–433, 2015.

[9] M. A. Yahaya, D. Ruan, G. Lu, and M. S. Dargusch, “Response of aluminium honeycomb sandwich panels subjected to foam projectile impact - An experimental study,” Int. J. Impact Eng., vol. 75, pp. 100–109, 2015.

[10] S. Li, X. Li, Z. Wang, G. Wu, G. Lu, and L. Zhao, “Finite element analysis of sandwich panels with stepwise graded aluminum honeycomb cores under blast loading,” Compos. Part A Appl. Sci. Manuf., vol. 80, pp. 1–12, 2016.

[11] P. Liu, Y. Liu, and X. Zhang, “Internal-structure-model based simulation research of shielding properties of honeycomb sandwich panel subjected to high-velocity impact,” Int. J. Impact Eng., vol. 77, pp. 1–14, 2015.

[12] D. Zhang, D. Jiang, Q. Fei, and S. Wu, “Experimental and numerical investigation on indentation and energy absorption of a honeycomb sandwich panel under low-velocity impact,” Finite Elem. Anal. Des., vol. 117, pp. 21–30, 2016.

[13] T. Boonkong, Y. O. Shen, Z. W. Guan, and W. J. Cantwell, “The low velocity impact response of curvilinear-core sandwich structures,” Int. J. Impact Eng., vol. 93, pp. 28–38, 2016.

[14] I. Dayyani, A. D. Shaw, E. I. Saavedra Flores, and M. I. Friswell, “The mechanics of composite corrugated structures: A review with applications in morphing aircraft,” Compos. Struct., vol. 133, pp. 358–380, 2015.

[15] J. Liu, S. Pattofatto, D. Fang, F. Lu, and H. Zhao, “Impact strength enhancement of aluminum tetrahedral lattice truss core structures,” Int. J. Impact Eng., vol. 79, pp. 3–13, 2015.

[16] C. Liu and F. Li, “Impact transient response in lattice sandwich panels under various boundaries using

reverberation ray matrix method," Compos. Struct., vol. 125, pp. 239–246, 2015.

[17] S. Li, F. Jin, W. Zhang, and X. Meng, "Research of hail impact on aircraft wheel door with lattice hybrid structure," J. Phys. Conf. Ser., vol. 744, p. 12102, Sep. 2016.

[18] S. Nemat-Nasser, W. J. Kang, J. D. McGee, W. G. Guo, and J. B. Isaacs, "Experimental investigation of energy-absorption characteristics of components of sandwich structures," Int. J. Impact Eng., vol. 34, no. 6, pp. 1119–1146, 2007.

[19] F. Yang, W. Niu, L. Jing, Z. Wang, L. Zhao, and H. Ma, "Experimental and numerical studies of the anti-penetration performance of sandwich panels with aluminum foam cores," Acta Mech. Solida Sin., vol. 28, no. 6, pp. 735–746, 2015.

[20] C. Liu, Y. X. Zhang, and L. Ye, "High velocity impact responses of sandwich panels with metal fibre laminate skins and aluminium foam core," Int. J. Impact Eng., vol. 100, pp. 139–153, 2017.

[21] V. Crupi, E. Kara, G. Epasto, E. Guglielmino, and H. Aykul, "Prediction model for the impact response of glass fibre reinforced aluminium foam sandwiches," Int. J. Impact Eng., vol. 77, pp. 97–107, 2015.

[22] L. Wan, Y. Huang, S. Lv, and J. Feng, "Fabrication and interfacial characterization of aluminum foam sandwich via fluxless soldering with surface abrasion," Compos. Struct., vol. 123, pp. 366–373, 2015.

[23] S. Gaitanaros and S. Kyriakides, "On the effect of relative density on the crushing and energy absorption of open-cell foams under impact," Int. J. Impact Eng., vol. 82, pp. 3–13, 2015.

[24] I. Elnasri and H. Zhao, "Perforation of Aluminum Foam Core Sandwich Panels under Impact Loading: A Numerical Study," in Design and Modeling of Mechanical Systems - II: Proceedings of the Sixth Conference on Design and Modeling of Mechanical Systems, CMSM 2015, March 23-25, Hammamet, Tunisia, M. Chouchane, T. Fakhfakh, H. Ben Daly, N. Aifaoui, and F. Chaari, Eds. Cham: Springer International Publishing, 2015, pp. 387–396.

[25] G. Zhang, B. Wang, L. Ma, L. Wu, S. Pan, and J. Yang, "Energy absorption and low velocity impact

response of polyurethane foam filled pyramidal lattice core sandwich panels," Compos. Struct., vol. 108, no. 1, pp. 304–310, 2014.

[26] M. Ghalami-Choobar and M. Sadighi, "Investigation of high velocity impact of cylindrical projectile on sandwich panels with fiber-metal laminates skins and polyurethane core," Aerosp. Sci. Technol., vol. 32, no. 1, pp. 142–152, 2014.

[27] J. Zhou, Z. W. Guan, W. J. Cantwell, and Y. Liao, "The energy-absorbing behaviour of foam cores reinforced with composite rods," Compos. Struct., vol. 116, no. 1, pp. 346–356, 2014.

[28] V. Anes, M. J. Freitas, L. Sousa, and L. Reis, "Impact damage characterization of sandwich panels produced with cork and pvc types of core," in 10th International Conference on Composite Science and Technology, 2015.

[29] I. Taraghi and A. Fereidoon, "Non-destructive evaluation of damage modes in nanocomposite foam-core sandwich panel subjected to low-velocity impact," Compos. Part B Eng., vol. 103, pp. 51–59, 2016.

[30] R. Nasirzadeh and A. R. Sabet, "Influence of nanoclay reinforced polyurethane foam toward composite sandwich structure behavior under high velocity impact," J. Cell. Plast., vol. 52, no. 3, pp. 253–275, Nov. 2014.

[31] D. Frich, J. Economy, "Thermally Stable Liquid Crystalline Thermosets Based on Aromatic Copolyesters: Preparation and Properties", J. Polym. Sci. A Polym. Chem., 35: 1061–1067, (1997).

[32] D. Frich, J. Economy, "Novel High-Temperature Aromatic Copolyester Thermosets: Synthesis, Characterization, and Physical Properties", Macromolecules 29: 7734-7739, (1996).

[33] Z. Parkar, Z. Parkar, C. Mangun, D. King, T. Field, G. Sutton, J. Economy, "Ablation characteristics of an aromatic thermosetting copolyester/carbon fiber composite" J. Compos. Mater., 46: 1819-1830, (2012).

[34] D. Frich, J. Economy, K. Goranov, "Aromatic Copolyester Thermosets: High Temperature Adhesive

Properties", Poly. Eng. and Sci, 37: 541-548, (1997).

[35] B. Vaezian, J. Meyer, J. Economy, "Processing of aromastic thermosetting copolyesters into foams and bulk parts: characterization and mechanical properties", Polym. Adv. Technol., 27: 1006−1013, (2016).

[36] M. Bakir, J. Meyer, J. Economy, I. Jasiuk, "Heat-Induced Polycondensation Reaction with Self-Generated Blowing Agent Forming Aromatic Thermosetting Copolyester Foams", Macromolecules, 49: 6489–6496, (2016).

[37] M.Z. Hassan, Z.W. Guan, W.J. Cantwell, G.S. Langdon, G.N. Nurick, "The influence of core density on the blast resistance of foam-based sandwich structures", International Journal of Impact Engineering, 50 (2012) 9-16.

[38] R. Nasirzadeh, A.R. Sabet, "Study of foam density variations in composite sandwich panels under high velocity impact loading", International Journal of Impact Engineering 63 (2014) 129-139.